

# Occurrence and Ultrastructure of a Variant (*rho*) Form of *Mycoplasma*

J. E. PETERSON, A. W. RODWELL, AND E. SHIRLEY RODWELL

C.S.I.R.O. Division of Animal Health, Animal Health Research Laboratory, Private Bag No. 1, P.O., Parkville,  
Vic., Australia 3052

Received for publication 3 March 1973

The ultrastructure of a variant ( $\rho$ ) form of *Mycoplasma* is described. The  $\rho$ -forms are characterized by dark-ground light microscopy as relatively rigid, unbranched, filamentous organisms with discoidal swellings, and by electron microscopy by the presence of an intracytoplasmic axial fiber extending throughout the length of the cell and associated with a terminal structure of characteristic appearance. In negatively stained preparations the fiber presents a pattern of transverse light and dark major bands, the dark band being divided by a central minor light band. The periodicity of the banding varies from 12.0 to 14.5 nm, and the width of the fiber varies from 40 to 120 nm. The fiber appears to be composed of fibrils aligned parallel to the long axis. The evidence indicates that the fiber contains protein and is devoid of nucleic acid.  $\rho$ -Forms were commonly found in *Mycoplasma* strains derived from goats and occasionally in bovine strains. They may have a wider distribution, as the growth medium was shown to be important both for the expression of the  $\rho$ -character and for the selection of the  $\rho$ -variant. The functional significance, if any, of the fiber and the terminal structure is unknown.

The ultrastructure of a number of species of *Mycoplasma* has been examined and has been the subject of recent reviews (1, 10). More recently, Rodwell et al. (18) briefly described a previously unrecorded morphological form characterized by dark-ground light microscopy as a pleomorphic, relatively rigid, filamentous organism with discoidal swellings, and by electron microscopy by the presence of an intracytoplasmic, banded, axial fiber. These variants, designated *rho* ( $\rho$ )-forms, were observed in cultures derived from strain V5 of *M. mycoides* var. *mycoides* and in strain Y *Mycoplasma*, which had originally been isolated from fibrinous peritonitis in a goat (13) and which is related serologically to *M. mycoides* var. *mycoides*.

The morphology of the  $\rho$ -form and the structure of its characteristic inclusion are now described more fully, together with observations on the occurrence of this form in other mycoplasma species, especially those of bovine and caprine origin.

## MATERIALS AND METHODS

The strains of mycoplasma examined and their origins are listed in Table 1. The medium used in most studies was the partly defined C2 medium (18)

or BVF-OS medium (19) supplemented with glucose, glycerol, and oleate (17). For some work the medium used was BVF-PS, which was similar to the supplemented BVF-OS except that ox serum (OS) was replaced by pig serum (PS). PPLO medium (Difco) supplemented by pig serum, yeast extract, and deoxyribonucleic acid (DNA) (PPLO-PS medium) was also used, particularly for the maintenance of mycoplasma strains.

For electron microscopy of whole cells, the basic method of preparation was as follows. Cultures were centrifuged and suspended in a solution (NPM) containing 0.25 M NaCl, 0.01 M MgSO<sub>4</sub>, and 0.02 M phosphate (pH 7.0), at 0 C. Formaldehyde or glutaraldehyde solutions were added to give a final concentration of the fixative of 4% (wt/vol). After fixation at 0 C for 2 to 16 h, the mycoplasmas were centrifuged and suspended in water. When it was desired to obtain an even and representative distribution of cells on the electron microscope grid, a pseudoreplication technique was used. Drops of cell suspension were applied to the surface of 2% Noble agar (Difco) plates. After the suspending medium had been absorbed, the cells were stripped from the agar surface on a parlodion film which was then transferred to a parlodion-carbon coated grid. For other examinations the fixed cell suspension was applied directly to the coated grid and the excess was removed by filter paper. To stain cells negatively, a drop of stain solution was applied to the preparation on the specimen grid, and after about 30 s

the excess was removed by filter paper. The most frequently used negative stains were 2% potassium phosphotungstate, 2% ammonium molybdate, or 1% uranyl acetate. As indicated in the text, other preparative methods were used for the examination of particular aspects of structure. Where appropriate, the effects of suspending and fixative solutions on cell morphology were monitored by the examination of freely floating organisms by dark-ground or phase-contrast light microscopy.

Cells to be sectioned were fixed in formaldehyde solution as above, sedimented by centrifugation, and suspended in a drop of 2% Noble agar. After secondary fixation in 1% osmium tetroxide in phosphate buffer (pH 7.2), the specimen blocks were dehydrated through graded ethanol and embedded in Araldite. Sections were double stained with lead and uranyl salts. Electron microscopy was performed with a Hitachi HU-11B instrument, and magnifications were calibrated by the use of a cross-line carbon grating replica with 2,160 lines per mm (Ernest F. Fullam, Inc.).

For autoradiography, pseudoreplicated preparations were coated with Ilford L4 photographic emulsion by a loop technique and subsequently developed in Kodak D19b solution.

The effects of protease treatment were examined in unfixed cells and in cells which had been fixed with formaldehyde and washed in 0.05 M tris(hydroxymethyl)-aminomethane-hydrochloride (pH 7.5). Cells were suspended at a density of approximately 1 mg (dry weight)/ml in 0.05 M phosphate buffer (pH 7.4) and the suspension was warmed to 37 C. Trypsin (Sigma Chemical Co.; 11,000 U/mg) or Pronase (Calbiochem; 45,000 proteolytic U/g) was added to a concentration of 0.1 mg/ml, and incubation continued for periods up to 18 h. The suspension was then chilled, and in most experiments formaldehyde was again added to a final concentration of 4%. The effect of the enzyme on the turbidity of the cell suspension was measured at 650 nm, and samples of treated cells were examined with an electron microscope.

Essentially the same procedure was used in the examination of the effects of nucleases, by using ribonuclease (Sigma Chemical Co.; 90 Kunitz U/mg protein) and deoxyribonuclease (Sigma Chemical Co.; 28,000 U/mg). When using deoxyribonuclease, 0.01 M MgSO<sub>4</sub> was added.

## RESULTS

**Distribution of  $\rho$ -forms. Species and strains of mycoplasmas in which  $\rho$ -forms were observed.** Mycoplasmas from several host species have been examined for the occurrence of  $\rho$ -forms. The results are shown in Table 1, which also shows the origin of all cultures examined. In unselected cultures, many of the caprine strains contained  $\rho$ -forms. In some they were the most abundant growth form, whereas in others they were rare. Similarly, in bovine strain 801, which is serologically related to *M. mycoides* var. *mycoides*,  $\rho$ -forms were abun-

TABLE 1. Occurrence of  $\rho$ -forms in mycoplasmas<sup>a</sup> grown in BVF-OS or BVF-PS media<sup>b</sup>

Mycoplasma strain	Country of origin	Reference <sup>c</sup>	$\rho$ -Forms <sup>d</sup>
<b>Bovine</b>			
<i>M. mycoides</i> var. <i>mycoides</i>			
PG1 (= 3278)	Not recorded	7	-
Gladysdale	Australia	12	-
V5	Australia	6	-
H22/1	Australia	18	+
<i>M. dispar</i>			
L2917	England	11	-
N29	Australia	5	+
801	Australia	e	+
<b>Caprine</b>			
Y	Australia	13, 18	+
Y2b	Australia	18	+
KH-1	Australia	e	+
PG3	Turkey	6, 7	+
Lister (pp goat)	Turkey	14	+
Smith	Turkey	6	+
BQT	Turkey	6	+
Cov. 3	Turkey	6	+
Ojo-1	Nigeria	e	+
Ojo-2	Nigeria	e	+
OSB-42	Nigeria	8	+
N108	Nigeria	8	+
Vom	Nigeria	5	-
G1/61	Sudan	8	-
Cal. goat	U.S.A.	12	+
<b>Ovine</b>			
<i>M. arginini</i> , G230	U.S.A.	7	-
<b>Avian</b>			
<i>M. gallisepticum</i> , S6	U.S.A.	9	-
<i>Acholeplasma laidlawii</i>			
Sewage A, PG8	England	7	-
Sewage B, PG9	England	14	-

<sup>a</sup> All strains listed here are from the collection maintained by G. S. Cottew at this laboratory.

<sup>b</sup> Several strains of mycoplasmas, including *M. bovis genitalium* (PG11), *M. bovis rhinitis* (PG43), *M. pneumoniae* (FH), and *M. gallisepticum* (QXO) are not included, as satisfactory growth was obtained only in PPLO-PS medium, which does not allow  $\rho$ -forms to develop.

<sup>c</sup> References were selected to give some indication of the origin and history of the strains examined, and in some cases, relationship to other mycoplasmas.

<sup>d</sup>  $\rho$ -Forms: +, observed; -, not observed, in cultures grown in BVF-OS or BVF-PS media. The relative abundance of  $\rho$ -forms, which varied greatly, is not indicated here as it is largely dependent on cultural conditions.

<sup>e</sup> G. S. Cottew (personal communication): 801, isolated from eye of cow; KH-1, isolated by K. L. Hughes from udder of goat; Ojo 1 and 2, isolated by M. O. Ojo from goats.

dant, whereas in arthritis strain L2917, they were rarely seen. We have not observed  $\rho$ -forms in the stock laboratory strains (V5, Gladysdale, PG1) of *M. mycoides* var. *mycoides* other than in the variants derived from V5. The morphology typical of this species in BVF-OS is shown in Fig. 1.

**Effects of medium on incidence of  $\rho$ -forms.** The isolation of  $\rho$ -forming variants Y2b and H22/1 from *Mycoplasma* strain Y and from the

V5 strain of *M. mycoides*, respectively, has been described (18). When subcultured from C2 medium, the  $\rho$ -form was initially the most abundant cell type when these strains were grown in BVF-OS medium, but the proportion diminished on repeated subculture. This effect was then examined more fully by using these two strains. The initial cultures of both strains contained some  $\rho$ -forms. Each strain was serially subcultured through C2 and BVF-OS media, changes in morphology being sought by dark-field light microscopy and electron microscopy.

In both strains, when maintained by passage in medium C2, the  $\rho$ -form rapidly became and then remained the predominant cell type (Fig. 2a). When passaged through liquid BVF-OS medium, the proportion of  $\rho$ -forms progressively diminished and by the sixth passage

accounted for only about 0.1% of the population (Fig. 2b). During six additional passages in BVF-OS medium, three of which were by means of single colonies on solid medium, the proportion of  $\rho$ -forms remained at about this low level. This was not a simple reversion to the morphology of the original culture, and the degree of pleomorphism was much reduced (cf. Fig. 1 and 2b). After this passaging through BVF-OS medium, the cultures were transferred back to C2 medium, in which they were maintained through an additional 11 passages. During this period, the proportion of  $\rho$ -forms progressively increased until it was again the predominant form (Fig. 2c, d). Both strains of mycoplasma behaved in a similar manner.

We did not observe  $\rho$ -forms in cultures in PPLO-PS medium, even with strains in which they were the predominant cell type when grown in BVF-OS or C2 medium, but the capacity to produce  $\rho$ -forms in BVF-OS medium was retained for at least two passages through PPLO-PS medium.

The incidence of  $\rho$ -forms is thus seen to be strongly influenced by the growth medium.  $\rho$ -Forms were abundant in cultures of some caprine strains of *Mycoplasma*, particularly in N108, Ojo-2, PG3, and OSB-42, grown in BVF-OS, even though these strains had not previously been cultivated in medium C2.

**Morphology and structure of the  $\rho$ -fiber.**  
**Whole cell preparations and isolated fibers.**  
 The  $\rho$ -form is characterized by the presence of an intracellular fiber ( $\rho$ -fiber) which exhibits a cross-banded structure. This fiber extends throughout the length of the cell as a single, continuous structure (Fig. 3). Where the cell diameter is relatively large, the  $\rho$ -fiber tends to curve gently in a more or less helical shape of no fixed pitch (Fig. 3b), but in thin filaments the fiber is straight (Fig. 3c). In suitable unfixed and unstained cells, the  $\rho$ -fiber can be faintly discerned by electron microscopy, but for adequate preservation and demonstration of structure it is necessary to use fixed cells, negatively stained. The appearance of the fiber under these conditions is not affected by the particular negative stain used (potassium phosphotungstate, ammonium molybdate, uranyl acetate).

Fibers could be prepared which were largely free of other cellular material by a procedure involving controlled tryptic digestion and sonic disruption of fixed cells. The morphology of the isolated fibers did not differ from that of the intracellular fibers and served to confirm that the detail observed was not due to overlying cytoplasmic or membranous material.



FIG. 1. *M. mycoides* var. *mycoides* grown in BVF-OS medium, showing its typical pleomorphic morphology. The filaments were flexible and the swellings were spheroidal. No  $\rho$ -forms were present. Electron micrograph of fixed, unstained culture. Bar represents 1  $\mu$ m.

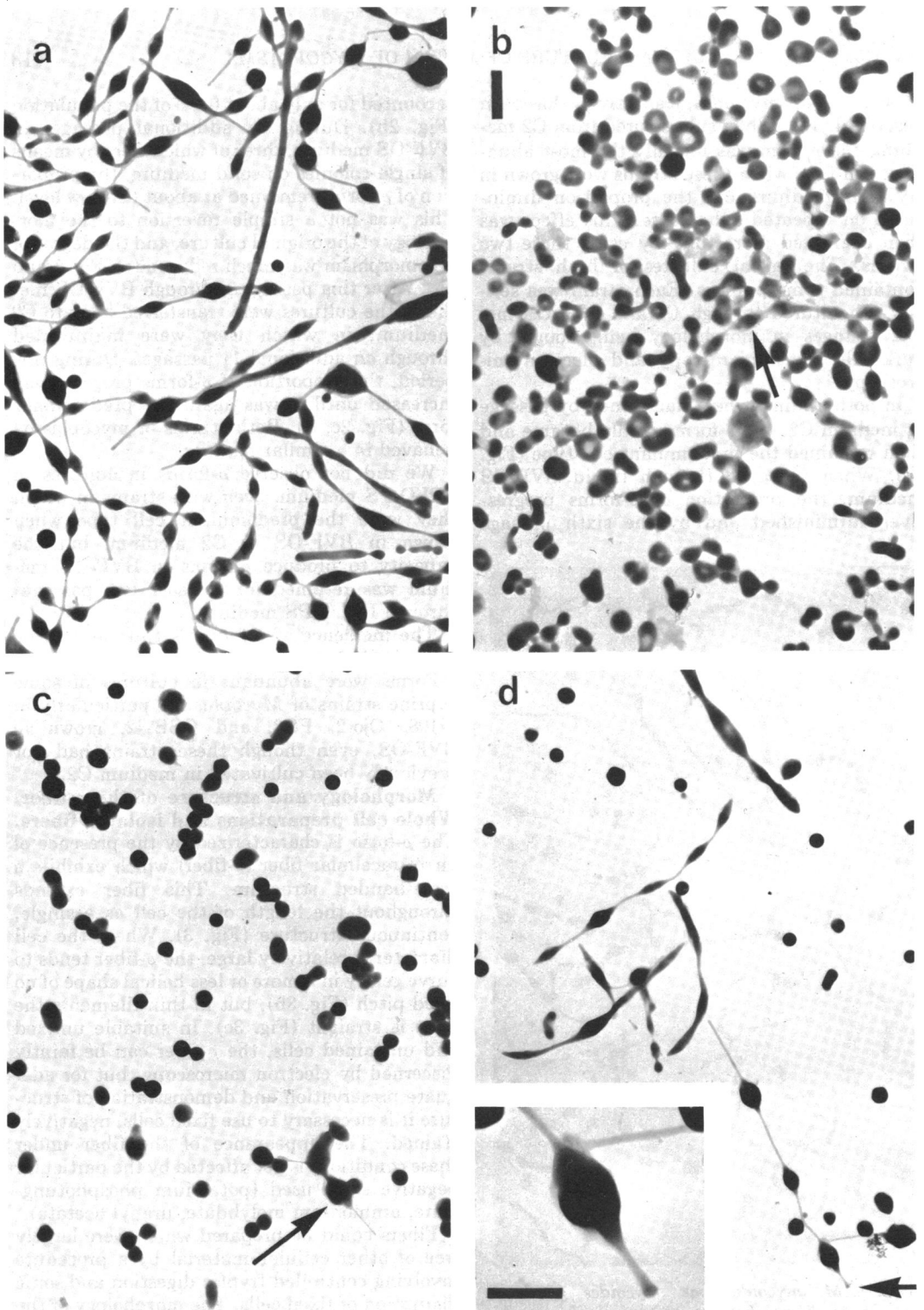


**FIG. 2.** Effect of medium on the incidence of  $\rho$ -forms in the H22/1 strain of *Mycoplasma* grown in C2 and BVF-OS media. Electron micrographs of fixed, unstained cultures. Bar represents 1  $\mu\text{m}$ . (a) After serial subculture in C2 medium, almost all cells were of the  $\rho$ -form; the filaments tended to be rigid and the swellings tended to be discoidal. (b) Culture was then transferred to BVF-OS medium and was serially subcultured in this.  $\rho$ -Forms (arrow) were rare, but the morphology had not reverted to that of the original non- $\rho$ -culture shown in Fig. 1. (c) Culture was then transferred back to C2 medium. On first subculture a few short  $\rho$ -forms (arrow) were present. (d) At the sixth subculture in C2 medium,  $\rho$ -forms were again becoming the dominant form. All the elongated cells are  $\rho$ -forms. Arrow indicates knoblike terminal structure shown at higher magnification in the inset (bar represents 0.5  $\mu\text{m}$ ).

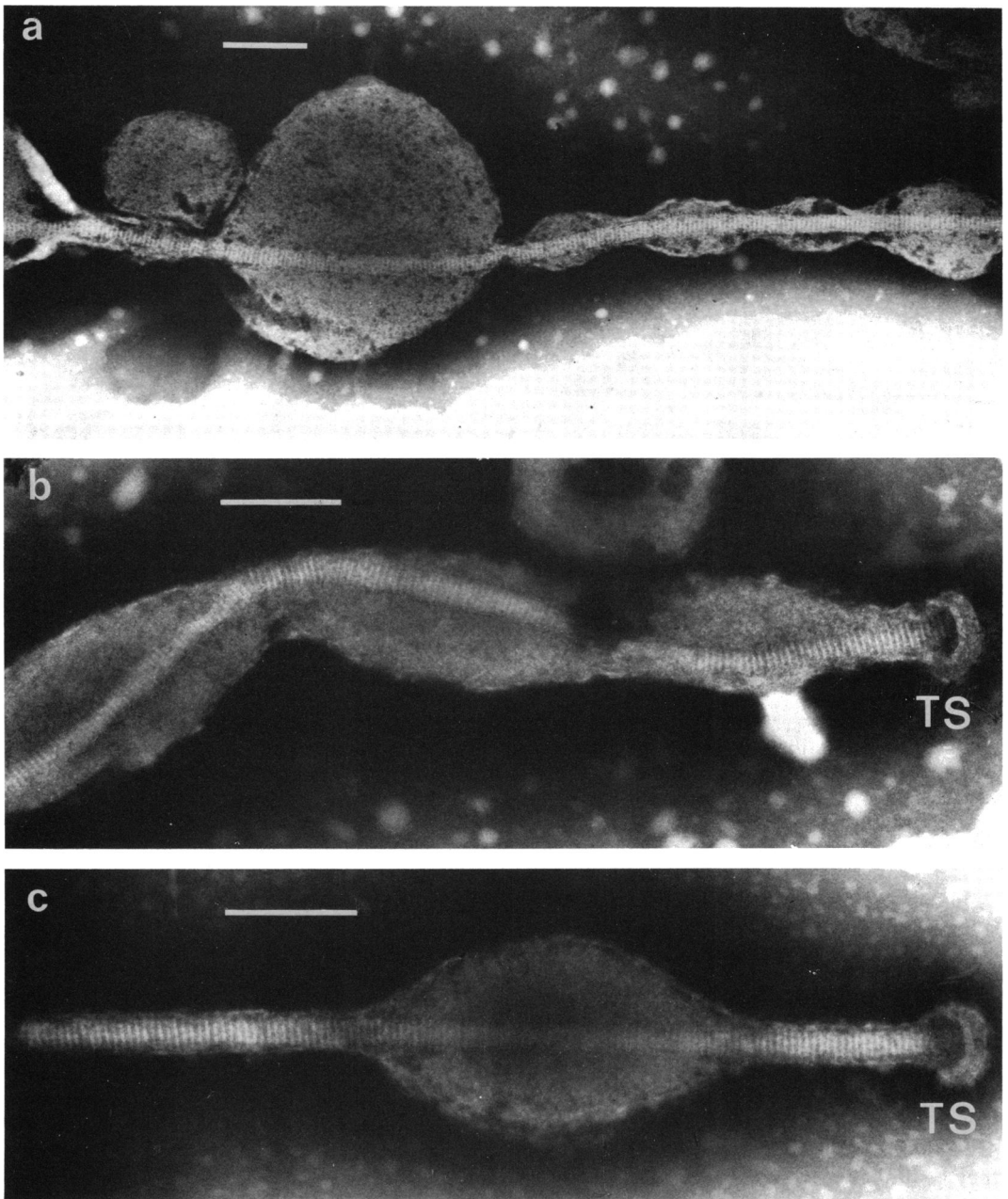


FIG. 3. Continuity of the  $\rho$ -fiber throughout the length of the cell is shown in  $\rho$ -forms of differing morphology. In (b) the fiber tends to form a loose helix. In (c), which is typical of the rigid filaments composed of discoidal swellings connected by a slender thread, the fiber is straight. Terminal structures (TS) are present in (b) and (c). Fixed, negatively stained. Bar represents 200 nm.

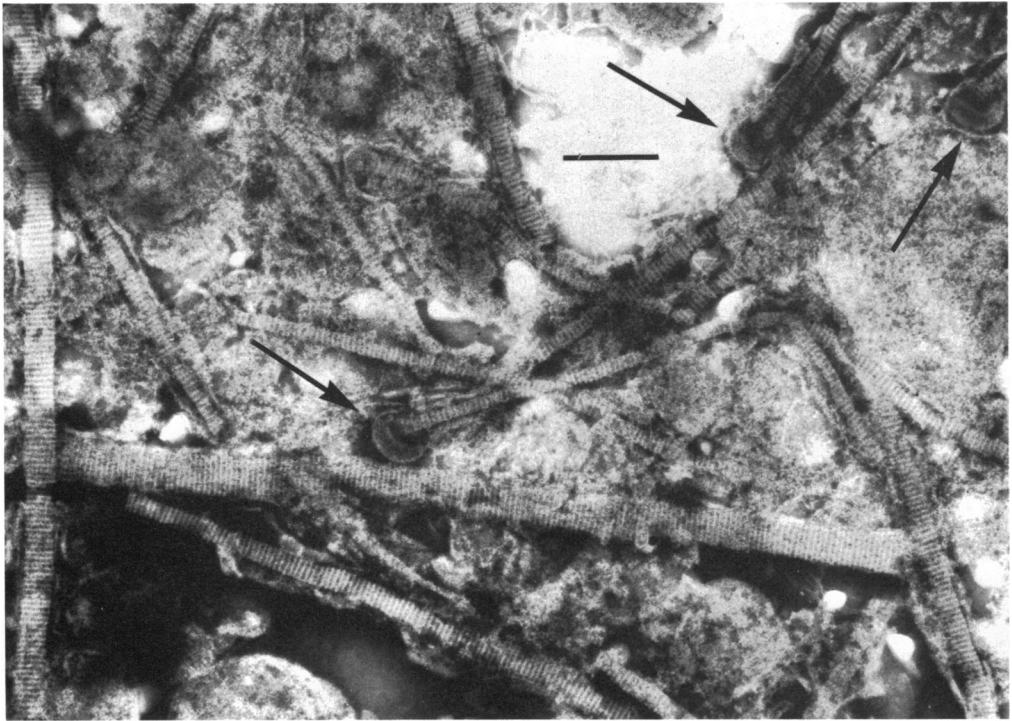


FIG. 4.  $\rho$ -Fibers partially isolated from fixed cells by protease treatment. Note the range in the width of the fibers and the retention of the TS (arrows) at the end of several fibers. Negatively stained. Bar represents 200 nm.

In negatively stained preparations, the diameter of the  $\rho$ -fiber varies between cells (Fig. 4), from about 40 to 120 nm, and to a lesser extent within a single cell.

Each  $\rho$ -fiber presents a pattern of transverse light and dark major bands, the dark band being divided by a central light minor band (Fig. 5). The periodicity of the banding, measured in a representative series of organisms, varied from 12.1 to 14.5 nm and was not significantly different between fixed and unfixed cells. The major light band measured 6.3 to 8.4 nm in width, along the axis of the fiber, and the dark band measured 5.2 to 6.3 nm. Although the alignment of the bands was usually orthogonal to the longitudinal axis of the fiber, variations did occur and in some segments they could be found tilted. Occasionally several segments, each tilted at a different angle, could be seen in a single fiber (Fig. 6).

In addition to the transverse banding pattern, striations could be seen parallel to the long axis of the fiber (Fig. 7). These striations appeared to be due to parallel-aligned fibrils about 3.0 nm diameter and tended to give a beaded appearance to the minor light band (Fig. 5, 7).

The  $\rho$ -fiber was completely intracytoplasmic,

and no evidence was seen of any limiting membrane. Fibers were never seen to branch, and the only variation from a single fiber that was seen was a partial longitudinal separation into two parallel fibers.

**Sectioned organisms.** In sections of Araldite-embedded cells, the  $\rho$ -fibers showed some differences from those in the negatively stained preparations. In longitudinal sections that had been postfixed in osmium and stained by lead and uranyl salts, the  $\rho$ -fiber showed the same general banding pattern (Fig. 8), although the minor light band was difficult to demonstrate. The most frequent periodicity of the banding was about 10.0 nm, with a range of about 9.0 to 12.5 nm. In transverse section (Fig. 9, 10), the  $\rho$ -fibers were evident as relatively translucent areas of more or less circular outline. The boundary of the fiber was not sharply defined, and in most fibers no internal structure could be resolved. Occasionally it was possible to distinguish a few circular profiles of about the same diameter as the longitudinal fibrils seen in negatively stained material, but of such low contrast as to preclude satisfactory examination.

**Stability of the  $\rho$ -fiber.** In the unfixed cell,

the  $\rho$ -fiber was very sensitive to osmotic effects, and any treatment which caused swelling of the unfixed cell led to the disappearance of the fiber. For example, cultures of filamentous  $\rho$ -forms were suspended in NPM solution and the osmolarity was varied by altering the concentration of NaCl; fixative was then added to the solution and the cells were examined by electron microscopy. A few osmotically swollen cells appeared when the NaCl concentration was reduced to 0.1 M, and the proportion of affected cells increased progressively with decreasing molarity until almost all cells were swollen at an NaCl concentration of 0.025 M. However, in all solutions, and even when suspended in distilled water, a few cells resisted osmotic swelling. In slightly or moderately swollen cells, the  $\rho$ -fiber remained discernible and its periodicity remained unaltered. Because of the irregular manner in which the filamentous cells changed shape as they became swollen, the enclosed  $\rho$ -fiber became irregularly twisted and folded within the swollen segment. Under these conditions the appearance of the fiber was that of rigid segments with sharp, angular bends at which the fiber split transversely across most of its width (Fig. 11). In more completely swollen cells, the  $\rho$ -fibers were rarely seen, but if present they retained their normal appearance. When cells were first swollen osmotically and then returned to an isotonic medium before being

fixed, they did not return to their original shape but became irregularly crenated and folded. However, the  $\rho$ -fiber again became demonstrable, although no longer co-incident with the long axis of the cell, and fibers retained many of their angular bends.

The effect of osmotic swelling on the appearance of the  $\rho$ -fiber was confirmed by suspending unfixed cells in varying concentrations (1 to 6%) of ammonium molybdate solution, which also served as a negative stain. Again, osmotic swelling and disruption of cells were correlated with the loss of the  $\rho$ -fiber as a discernible entity.

The effects of the ionic or nonionic nature of the solute and of  $Mg^{2+}$  concentration were examined by suspending cells in modifications of NPM. Neither replacement of NaCl by equimolar concentrations of sucrose nor reduction of the  $Mg^{2+}$  concentration affected the structure or stability of the  $\rho$ -fiber other than through osmotic effects, although the omission of  $Mg^{2+}$  reduced the stability of the plasma membrane.

After cells had been fixed by formaldehyde or glutaraldehyde, they were no longer susceptible to osmotic swelling and retained essentially the same morphology seen in unfixed preparations by dark-ground light microscopy. The  $\rho$ -fiber was also stabilized by fixation and could be isolated and washed without apparent alteration.

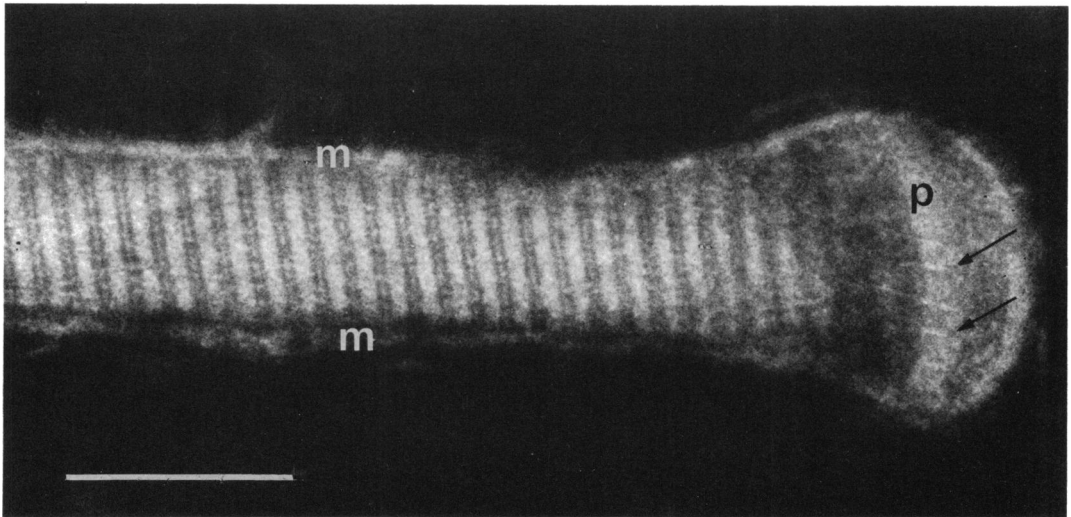


FIG. 5. Filamentous terminal portion of  $\rho$ -form cell showing detail of the fiber and the terminal structure. The fiber almost completely fills the plasma membrane (m) in this portion of the cell. The minor light band which divides the dark major band is somewhat beaded in appearance, and suggestions of longitudinal striations are evident in some areas. The  $\rho$ -fiber ends at the broad, electron-translucent plate (p) of the TS. Several longitudinal fibrils (arrows) penetrate this plate. Fixed cell, negatively stained. Bar represents 100 nm.

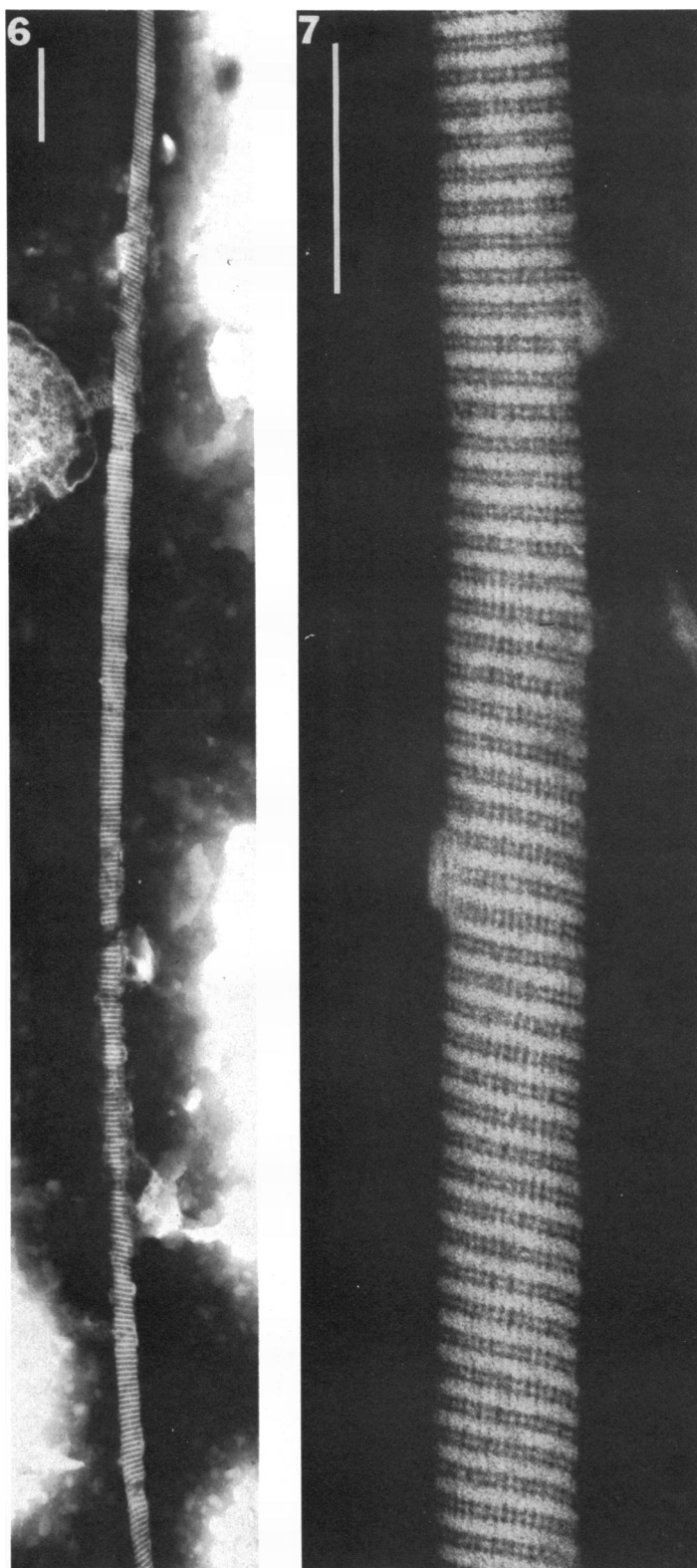


FIG. 6. Isolated  $\rho$ -fiber showing variability in the angle at which the cross striations lie in relation to the long axis. Some variation in periodicity is also evident. Negatively stained. Bar represents 200 nm.

FIG. 7. Isolated  $\rho$ -fiber, showing detail of its structure. The tilting of the cross-banding in portion of fiber shown here is apparently due to slight alterations in the register of adjacent longitudinal fibrils. Fiber isolated from fixed cell by protease and ultrasonic treatment, negatively stained. Bar represents 100 nm.



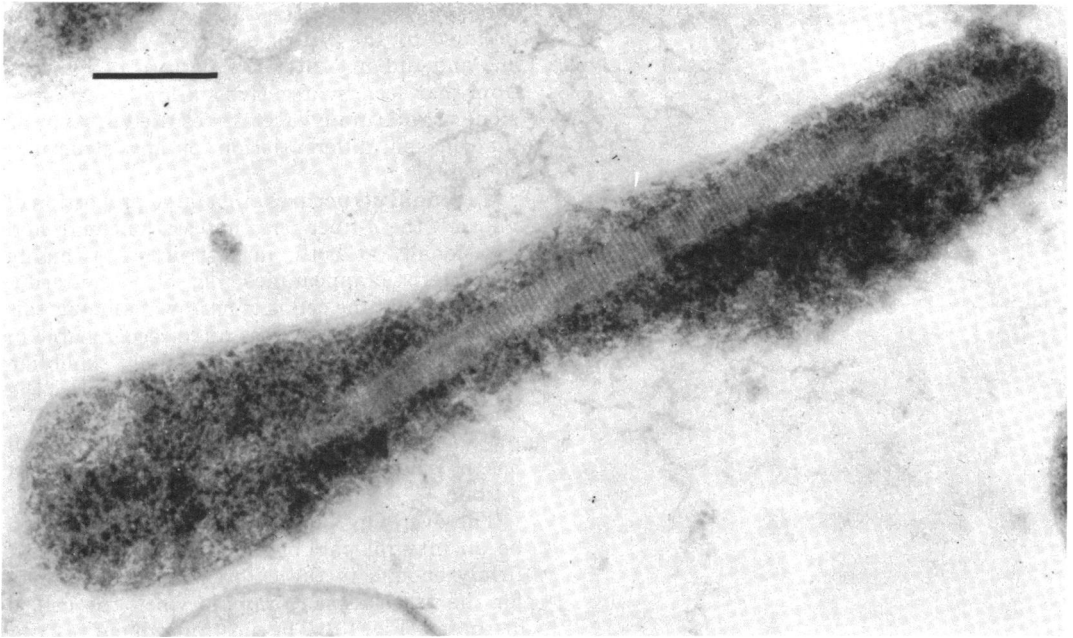


FIG. 8. Longitudinal section through  $\rho$ -form, and its fiber. Uranyl and lead stain. Bar represents 200 nm.

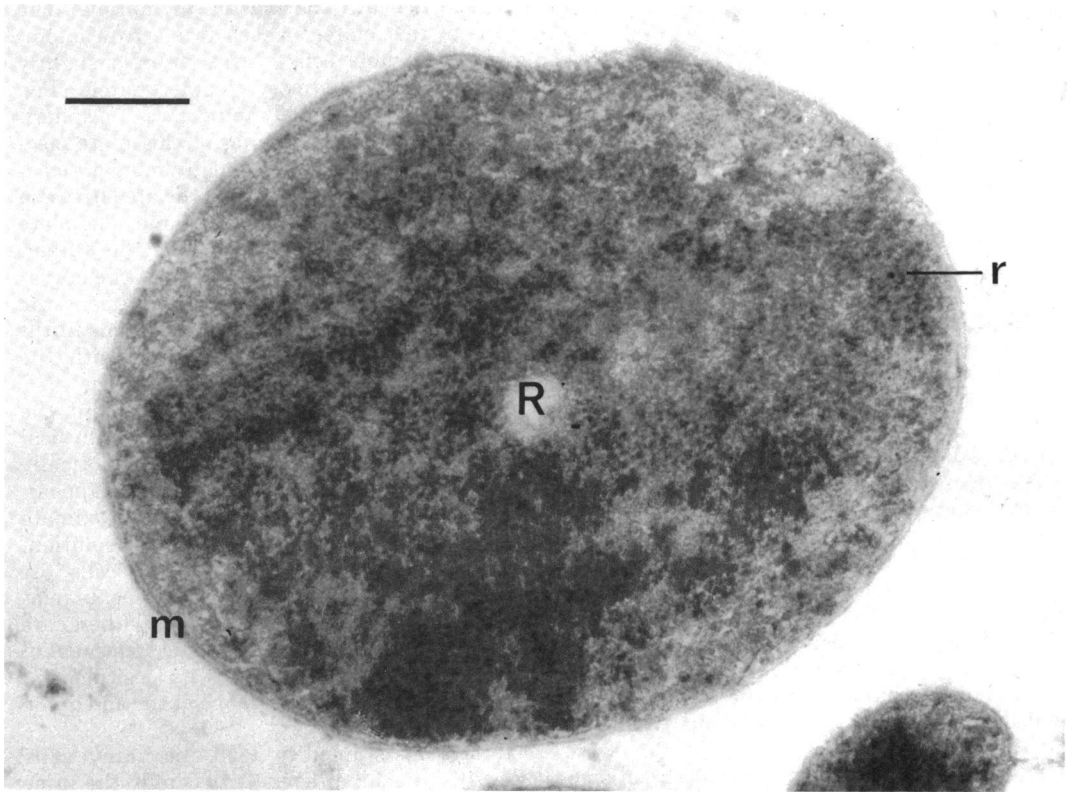


FIG. 9. Transverse section of  $\rho$ -form, showing plasma membrane (m), ribosomes (r), and  $\rho$ -fiber (R). No structural detail of the fiber can be resolved. Uranyl and lead stain. Bar represents 200 nm.

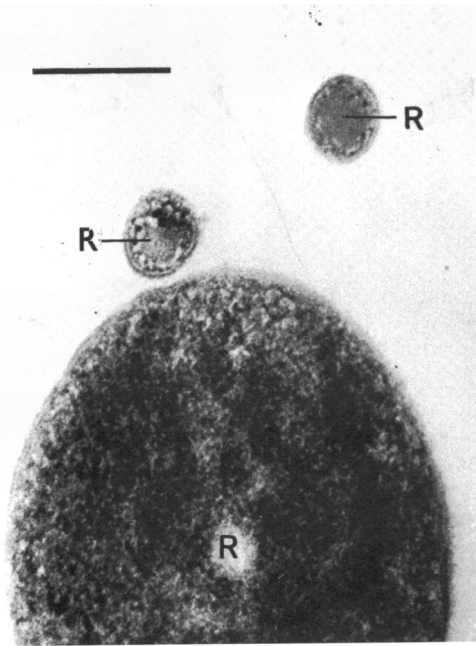


FIG. 10. Transverse sections of  $\rho$ -forms. The large figure is comparable to Fig. 9 and has been cut through a swollen portion of the cell. The two small sections have been cut through the thin threadlike portions of the cell and show the cytoplasmic space to be almost completely filled by the  $\rho$ -fiber (R). Uranyl and lead stain. Bar represents 200 nm.

**Composition of the  $\rho$ -fiber.** The study of the effects of enzymes or chemical reagents on the  $\rho$ -fiber in unfixed cells is limited by the instability of the fiber as a recognizable structure once the cell becomes osmotically damaged, and by the probable lack of contact between fiber and reagent in undamaged cells. When Formalin- or glutaraldehyde-fixed cells were exposed to the action of trypsin or Pronase for several hours, the  $\rho$ -fibers became eroded, lost their banding pattern, and finally were completely disintegrated. Under the same conditions ribonuclease, deoxyribonuclease, detergents, and lipid solvents were without demonstrable effect on the structure of the  $\rho$ -fiber.

Autoradiographs of cells in which the DNA was uniformly labeled by growth with  $^3\text{H}$ -thymidine showed (Fig. 12) that labeling was restricted to the swollen portions in  $\rho$ -forms of the beaded type. The threadlike connecting portions of the filament and the terminal knoblike swellings were unlabeled and thus were apparently free of DNA.

The isolated  $\rho$ -fibers have not been satisfactorily stained. Phosphotungstic acid and uranyl

acetate, when used as positive stains, were retained by the  $\rho$ -fiber only very slightly, if at all, and did not alter the pattern of banding from that seen by negative staining. Lead salts alone or with uranyl acetate resulted in staining that lacked differentiation of any structural elements.

**Terminal structures.** In a large proportion of  $\rho$ -forms, the  $\rho$ -fiber terminates at one end, and occasionally at both, in a structure of highly characteristic appearance (Fig. 5). If the terminal portion of the cell is of narrow diameter, this terminal structure (TS) is often recognizable in unstained preparations as a slight knoblike swelling (Fig. 2d), but where the diameter of the terminal portion of the cell is greater, the TS may only be recognized when stained. The TS has not been observed without an associated  $\rho$ -fiber.

The overlying plasma membrane appears to be an integral part of the TS and is attached firmly enough to the cytoplasmic components for the association to remain when the cell is disrupted (Fig. 13). The most prominent feature of the TS in negatively stained preparations is an electron-translucent plate which lies a short distance beneath the plasma membrane. The shape of this plate, as seen in electron micrographs of whole cells, varies from a slightly curved arc to an almost complete circle (Fig. 14), which is presumably indicative of a spherical structure. On both sides of this plate electron opacity is increased, usually more noticeably on the internal side than in the area between the plate and the plasma membrane. The plate covers an area slightly wider than the  $\rho$ -fiber, the end of which is contained within the curvature of the plate. In occasional specimens the plate is seen to be traversed by a few fine fibrils (Fig. 5) which may be continuous with the longitudinal fibrils of the  $\rho$ -fiber (Fig. 7).

The association between the TS and the  $\rho$ -fiber is close and possibly due to physical attachment. When  $\rho$ -forms are osmotically swollen, both the TS and the  $\rho$ -fiber disappear. When the cells are returned to the approximate isotonic conditions provided by NPM solution, both re-appear, and although the cells are distorted, the  $\rho$ -fiber invariably retains its relationship to the TS. Also, when  $\rho$ -fibers are isolated by protease and ultrasonic treatment of fixed cells, the TS maintains its position and essential structural appearance at the end of the fiber (Fig. 4, 13, 15).

In sections stained by lead and uranyl salts (Fig. 16), the TS appears structurally the same as in negatively stained preparations, except

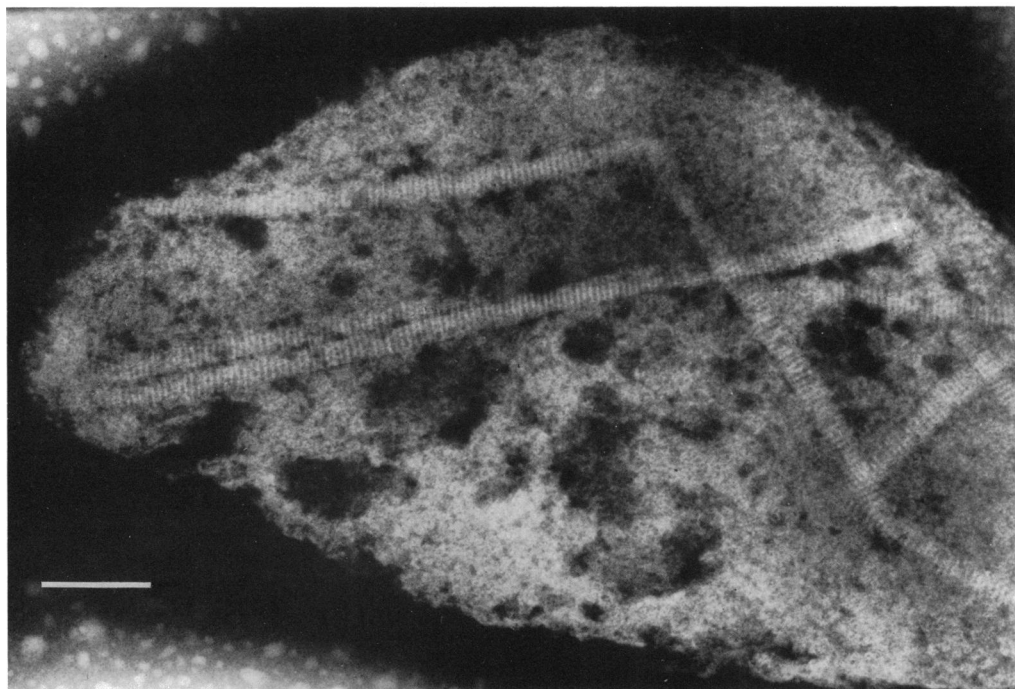


FIG. 11.  $\rho$ -Form filamentous cell swollen osmotically before being fixed. Note the angular fractures and irregular folding of the fiber. Negatively stained. Bar represents 200 nm.

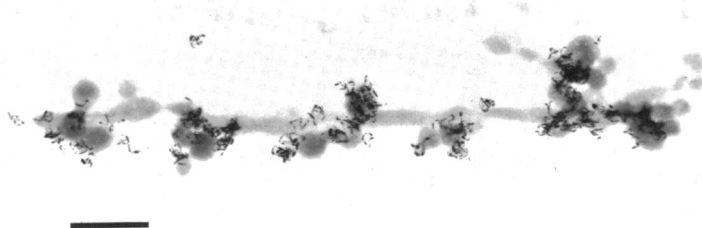


FIG. 12. Autoradiograph of  $\rho$ -form grown in the presence of  $^3\text{H}$ -thymidine. The absence of DNA from the  $\rho$ -fiber is indicated by the absence of developed silver grains over the filamentous regions of the cell; its presence is restricted to the swollen regions of the cell. Bar represents 1  $\mu\text{m}$ .

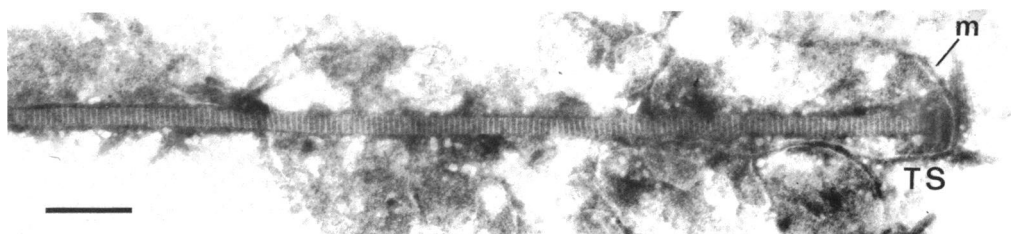


FIG. 13.  $\rho$ -Fiber partially isolated from fixed cell by protease and ultrasonic treatment. The TS remains attached to the fiber, and the plasma membrane (m) retains its attachment over the TS region. Negatively stained. Bar represents 200 nm.

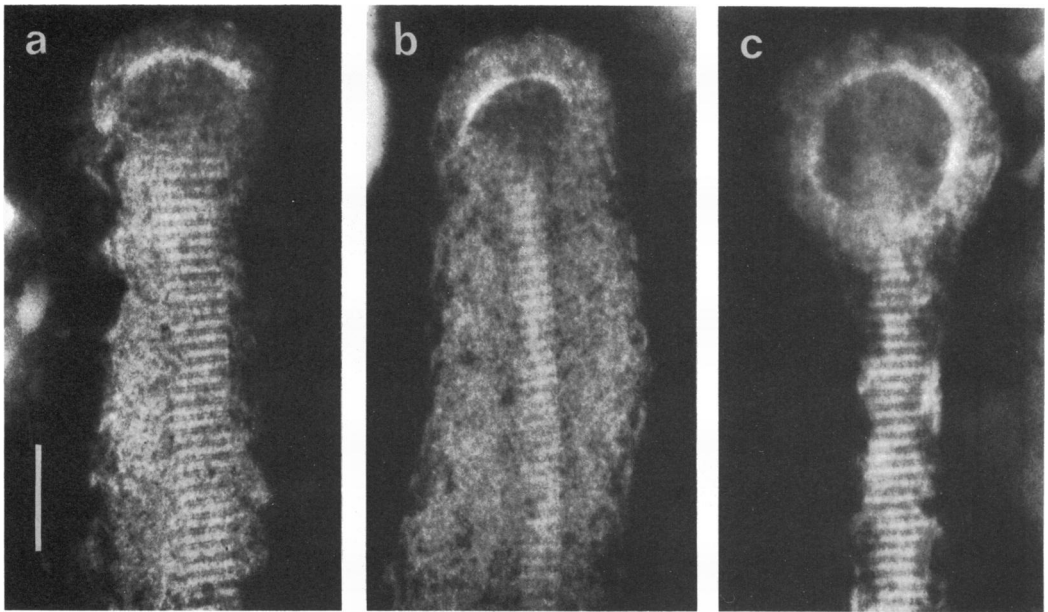


FIG. 14. Morphological variations in the TS. The prominent electron-translucent plate varies from slightly curved as in (a) to spherical as in (c). The end of the  $\rho$ -fiber lies within the curvature of this plate. Fixed cells, negatively stained. Bar represents 100 nm.

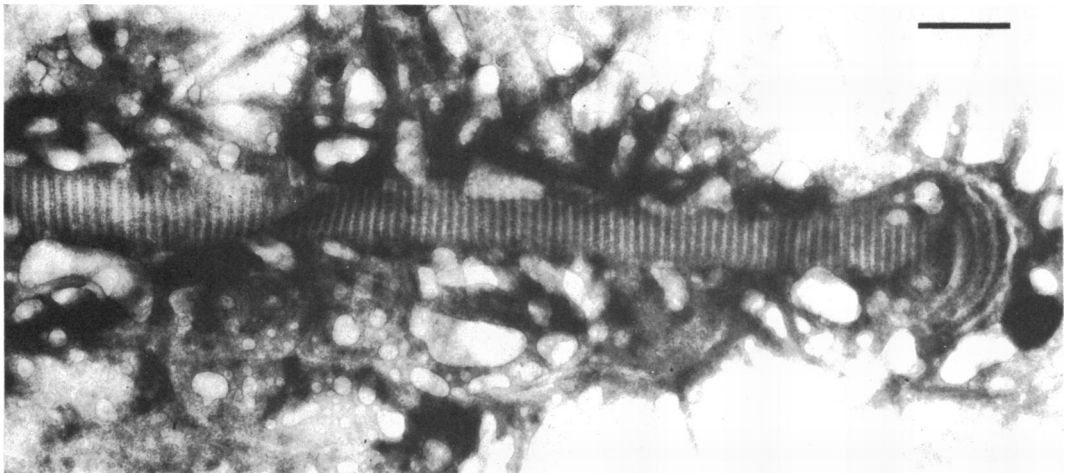


FIG. 15.  $\rho$ -Fiber isolated by protease digestion of fixed cell. The TS remains firmly attached and shows somewhat more complexity of structure than is apparent in less severely treated preparations, such as Fig. 13. Bar represents 100 nm.

that the translucent plate is much thinner and often difficult to define.

#### DISCUSSION

When examining the morphology of mycoplasmas, it is necessary to distinguish between true pleomorphism and distortion due to preparative technique. The subject has been discussed extensively by Freundt (10). It has been

our experience that the morphology observed in a culture of freely floating cells observed by dark-ground or phase-contrast light microscopy is most closely retained for electron microscope examination by fixation with formaldehyde or glutaraldehyde added either to the culture medium or to the cells suspended in NPM solution. In general, formaldehyde was preferred for giving cleaner preparations, especially in the pres-

ence of some serum-containing media. Distortion and shrinkage of cells appeared to be almost absent with this technique, whereas when reliance was placed on osmotic control only, without fixation (e.g., with the use of an appropriate concentration of ammonium molybdate negative-staining solution), a significant proportion of cells, in some strains of mycoplasmas, was always greatly distorted.

From comparisons of cells prepared by a number of techniques, it was concluded that some shrinkage occurred during dehydration and embedding in Araldite, and this reduced the periodicity of the  $\rho$ -fibers as seen in sections. Some flattening possibly occurred when whole fixed cells were dried on the specimen grid in the negatively stained preparations. It is unlikely that this would have resulted in any enlargement of the periodicity seen in long fibers, although it may have had some effect on the apparent width of fibers.

In addition to its use in monitoring electron microscope preparations for artifacts, the value of light microscope examination of wet preparations in morphological studies is stressed, as it is only by this technique that the relative rigidity

of the  $\rho$ -form and the discoid nature of the swollen areas of the cell can be readily demonstrated. In dried preparations, the disks tend to lie flat and their thin profile is not evident.

The incidence of  $\rho$ -forms is influenced by several factors, some nutritional, others probably genetic. In stock laboratory strains of *M. mycoides* var. *mycoides*,  $\rho$ -forms have not been observed, and isolations have been made only after adaptation to growth in C2 medium, their appearance coinciding with an increase in the growth rate of the culture (18). It seems likely that the initial appearance of  $\rho$ -forms, under these conditions, involved mutation and the selection of a faster growing genotype. Similar evidence is not readily available in relation to the mycoplasmas of caprine origin, as in these a high proportion of unselected cultures, with a wide geographical distribution, were observed to contain  $\rho$ -forms on first examination.

The composition of the medium has been shown to be an important factor in determining the proportion of  $\rho$ -forms in cultures of strain Y and the  $\rho$ -forming variants derived from strain V5. Growth in C2 medium consistently resulted in an increase in the proportion of  $\rho$ -forms,

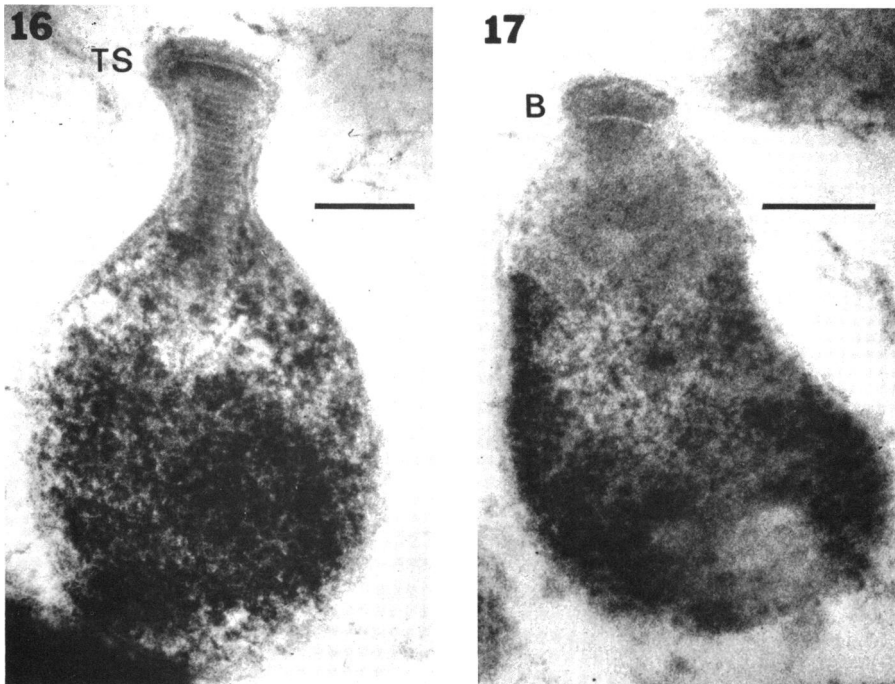


FIG. 16. Section of  $\rho$ -form cell cut longitudinally through the TS and portion of the fiber. Uranyl and lead stain. Bar represents 100 nm.

FIG. 17. Section of *M. gallisepticum* prepared as for Fig. 16. Note the morphological similarity of the "bleb" region (B) to the TS region shown in Fig. 16. Bar represents 100 nm.

whereas serial subculture in BVF-OS medium was accompanied by a diminution. As this fluctuation in the relative abundance of  $\rho$ -forms occurred progressively over several subculturing, and as the colonial form of the variant with a high proportion of  $\rho$ -forms presented no specific distinguishing characteristic, it could not be determined whether the effect was the result of selection for or against the  $\rho$ -form genotype or whether it was due to inhibition of the expression of the  $\rho$ -character. In contrast to this more gradual effect seen in C2 and BVF-OS media, the PPLO-PS medium had an immediate effect, as  $\rho$ -forms could be completely eliminated at the first subculture in this medium. Return to C2 medium, even after several subcultures in PPLO-PS medium, resulted in their immediate reappearance. These results are indicative of effects on the phenotypic expression and are clearly not due to genotype selection.

Investigation of the nutritional factors involved in the expression of the  $\rho$ -character has shown the essential requirements to be an unrestricted energy source and a medium of relatively high tonicity (Rodwell, Peterson, and Rodwell, Ann. N.Y. Acad. Sci., in press). Because of the limitations imposed by the factors discussed above and the difficulty of adapting some mycoplasmas to growth in particular media, it is not always possible to indicate whether an inability to produce  $\rho$ -forms is a genetic characteristic of a particular species or strain or whether expression of the character has been suppressed.

The morphogenesis of the  $\rho$ -form has not yet been elucidated. Association of the fiber with a terminal structure is a constant feature, and the latter may serve as a point of synthesis or assembly. The terminal structure shows some similarity to the "bleb" of *M. gallisepticum* (15), in so far as both structures are characterized by an electron-translucent plate situated beneath the plasma membrane and surrounded by zones of differential staining with electron-dense stains (Fig. 16, 17). In both cases the structures form well-defined terminal features in the cell. Biberfeld and Biberfeld (3) described a rather similar structure in *M. pneumoniae* which, in some cells, was associated with an electron-dense "rod" showing some indication of periodicity. The structural similarity of these features is sufficient to suggest a similarity in morphogenesis or function.

The chemical nature of the  $\rho$ -fiber is, at present, being investigated further. The results reported here indicate that it contains protein and is substantially free of nucleic acids. By

polyacrylamide gel electrophoresis, we found (Rodwell, Peterson, and Rodwell, Ann. N.Y. Acad. Sci., in press) a characteristic, prominent protein band which occurs only in cultures containing  $\rho$ -forms. Whether or not it is the structural protein of the  $\rho$ -fiber is yet to be determined. Although the fiber appears to be relatively rigid and unable to withstand sharp bending, the variability shown in its periodicity and the tilting sometimes seen in the bands suggest that some molecular movement is possible in the direction of the long axis of the fiber, possibly in a manner similar to that which occurs in contractile proteins.

No functional significance has yet been found for the  $\rho$ -fiber or its terminal structure. An association with cell attachment and motility seemed possible, in view of the type of motility described in other mycoplasmas (2, 4, 16), but we have not been able to demonstrate motility in  $\rho$ -forms. On the other hand, the  $\rho$ -fiber could simply be a para-crystalline aggregation of a cell protein synthesized in excess of the requirements of the cell.

#### ACKNOWLEDGMENT

We gratefully acknowledge the photographic work of Eric Smith.

#### LITERATURE CITED

1. Anderson, D. R. 1969. Ultrastructural studies of mycoplasmas and the L-phase of bacteria, p. 365-402. In L. Hayflick (ed.), *The Mycoplasmatales and the L-phase of bacteria*. Appleton-Century-Crofts, New York.
2. Andrewes, C. H., and F. V. Welch. 1946. A motile organism of the pleuropneumonia group. *J. Pathol. Bacteriol.* **58**:578-580.
3. Biberfeld, G., and P. Biberfeld. 1970. Ultrastructural features of *Mycoplasma pneumoniae*. *J. Bacteriol.* **102**:855-861.
4. Bredt, W. 1968. Motility and multiplication of *Mycoplasma pneumoniae*. A phase contrast study. *Pathol. Microbiol.* **32**:321-326.
5. Cottew, G. S., and R. H. Leach. 1969. Mycoplasmas of cattle, sheep, and goats, p. 527-570. In L. Hayflick (ed.), *The Mycoplasmatales and the L-phase of bacteria*. Appleton-Century-Crofts, New York.
6. Cottew, G. S., W. A. Watson, O. Erdag, and F. Arisoy, 1969. Mycoplasmas of caprine pleuropneumonia in Turkey and their relationship to other mycoplasmas of goats and *M. mycoides* var. *mycoides*. *J. Comp. Pathol.* **79**:541-551.
7. Edward, D. G., and E. A. Freundt. 1969. Classification of the *Mycoplasmatales*, p. 147-200. In L. Hayflick (ed.), *The Mycoplasmatales and the L-phase of bacteria*. Appleton-Century-Crofts, New York.
8. El Nasri, M. 1967. Mycoplasma from contagious caprine pleuropneumonia. *Ann. N.Y. Acad. Sci.* **143**:298-304.
9. Fabricant, J. 1969. Avian mycoplasmas, p. 621-641. In L. Hayflick (ed.), *The Mycoplasmatales and the L-phase of bacteria*. Appleton-Century-Crofts, New York.
10. Freundt, E. A. 1970. Morphology and ultrastructure of the mycoplasmas, p. 29-81. In J. T. Sharp (ed.), *The*

- role of mycoplasmas and L-forms of bacteria in disease. Thomas, Springfield, Ill.
11. Gourlay, R. N., and R. H. Leach. 1970. A new *Mycoplasma* species isolated from pneumonic lungs of calves (*Mycoplasma dispar* sp. nov.). *J. Med. Microbiol.* **3**:111-123.
  12. Hudson, J. R., G. S. Cottew, and H. E. Adler. 1967. Diseases of goats caused by *Mycoplasma*: a review of the subject with some new findings. *Ann. N.Y. Acad. Sci.* **143**:287-297.
  13. Laws, L. 1956. A pleuropneumonia-like organism causing peritonitis in goats. *Aust. Vet. J.* **32**:326-329.
  14. Lemcke, R. M. 1964. The serological differentiation of *Mycoplasma* strains (pleuropneumonia-like organisms) from various sources. *J. Hyg.* **62**:199-219.
  15. Maniloff, J., H. J. Morowitz, and R. J. Barnett. 1965. Ultrastructure and ribosomes of *Mycoplasma gallisepticum*. *J. Bacteriol.* **90**:193-204.
  16. Nelson, J. B., and M. J. Lyons. 1965. Phase-contrast and electron microscopy of murine strains of *Mycoplasma*. *J. Bacteriol.* **90**:1750-1763.
  17. Plackett, P., S. H. Buttery, and G. S. Cottew. 1963. Carbohydrates of some *Mycoplasma* strains, p. 535-547. In N. E. Gibbons (ed.), *Recent Progress in Microbiology*, Symposium held at the 8th International Congress of Microbiology, Montreal, 1962. University Press, Toronto.
  18. Rodwell, A. W., J. E. Peterson, and E. S. Rodwell. 1972. Macromolecular synthesis and growth of mycoplasmas, p. 123-139. In *Ciba Foundation Symposium: pathogenic mycoplasmas*. Associated Scientific Publishers, Amsterdam.
  19. Turner, A. W., A. D. Campbell, and A. T. Dick. 1935. Recent work on pleuro-pneumonia contagiosa boum in north Queensland. *Aust. Vet. J.* **11**:63-71.